

Magnetic Octupole Response of Dielectric Quadrumers

Pavel D. Terekhov,* Andrey B. Evlyukhin,* Dmitrii Redka, Valentyn S. Volkov, Alexander S. Shalin, and Alina Karabchevsky

The development of new approaches to tuning the resonant magnetic response of simple all-dielectric nanostructures is very important in modern nanophotonics. Here, it is shown that a resonant magnetic octupole (MOCT) response can be obtained by dividing a solid rectangular silicon block to a quadramer structure with the introduction of narrow gaps between four nanocubes. The spectral position of the MOCT resonance is controlled and tuned by varying the distance between the nanocubes. It is demonstrated that several magnetic hot-spots related to the MOCT resonance can be located in the gaps creating a strong magnetic field gradient in free space. It is observed that the resonant excitation of the MOCT moment leads to a significant enhancement of light absorption in the system at the spectral region, where light absorption in bulk silicon is weak. The results of this work can be applied to design new composite antennas and metamaterials based on complex building blocks, energy harvesting devices, and molecular trapping with magnetic hot-spots.

of electromagnetic energy.^[6–8] Additionally, dielectric high-index particles have commercial value due to low resonant absorption in optical range,^[9] while plasmonic structures experience significant Ohmic losses.^[10–12] To study scattering of light by dielectric nanostructures one can use the multipole decomposition approach, already widespread in scientific investigations^[13–26] including different spectral ranges.^[27,28] State-of-the-art literature reports that the multipole responses can be tuned by changing particles' geometry,^[29] size, aspect ratio, material dispersion, and the refractive index of surrounding media. Several recent studies have focused on high-order multipole excitations.^[30–34]

Owing to the large value of refractive index and low losses in near-infrared^[35] silicon is the most suitable material for

the resonant dielectric nanophotonics^[4] and structures development.^[36–39] For instance, silicon nanostrips placed on optical waveguide allows for probing forbidden overtone transitions.^[40] If placed on top of a lossy plasmonic material, silicon nanostrip allows for the realization of the cloaking effect and manipulation with waveguide's evanescent fields.^[41]

Dimers, oligomers, and other dielectric nanostructures (fabricated from silicon) are used for magnetic field concentration and enhancement.^[42,43] In this work we study the optical properties of the silicon quadramer which supports the resonant excitation of a magnetic octupole moment and allows it to be controlled using structure parameters. We show that a solid block of crystalline silicon does not support magnetic octupole resonances, and that simply cutting it enables a resonant magnetic octupole response of the resulting silicon quadramer.

This effect leads to both the magnetic field enhancement inside the structure's slits and to increased light absorption by the structure. The suggested structures can be used to design modern optical devices and for efficient light control using magnetic octupole excitation. It is worth noting, that the achieved magnetic octupole response appears in an unusual part of the spectrum: for a bulk structure of comparable size, it would appear at far shorter wavelengths.

Modern optics actively studies metasurfaces and metamaterials, which require advanced meta-atoms supporting a specially tuned optical response. High-order multipole excitations feature specific radiation patterns and distributions of near fields. Therefore, involving high-order multipoles in an optical response of metasurfaces can expand their functional properties.^[44] Usually,

1. Introduction


Dielectric nanophotonics is one of the most actively developing fields in photonics research.^[1–3] A variety of applications of dielectric nanostructures in technological devices has led to a growing interest of scientific groups over the globe. One very important property of dielectric structures in comparison to their metal counterparts is the opportunity to control electric and magnetic components of light due to the excitation of electric and magnetic multipole resonances^[4–6] with the simultaneous accumulation

P. D. Terekhov, Dr. A. Karabchevsky
School of Electrical and Computer Engineering
Ben-Gurion University
Beer-Sheva 8410501, Israel
E-mail: terekhovpd@gmail.com

P. D. Terekhov, Dr. A. B. Evlyukhin, Dr. A. S. Shalin
Department of Physics and Engineering
ITMO University
49 Kronversky Ave. St. Petersburg 197101, Russia
E-mail: a.b.evlyukhin@daad-alumni.de

Dr. A. B. Evlyukhin, Dr. V. S. Volkov
Moscow Institute of Physics and Technology
9 Institutsky Lane Dolgoprudny 141700, Russia

Dr. D. Redka
Department of Photonics
Saint Petersburg Electrotechnical University LETI
5 Prof. Popova Street St. Petersburg 197376, Russia

 The ORCID identification number(s) for the author(s) of this article can be found under <https://doi.org/10.1002/lpor.201900331>

DOI: 10.1002/lpor.201900331

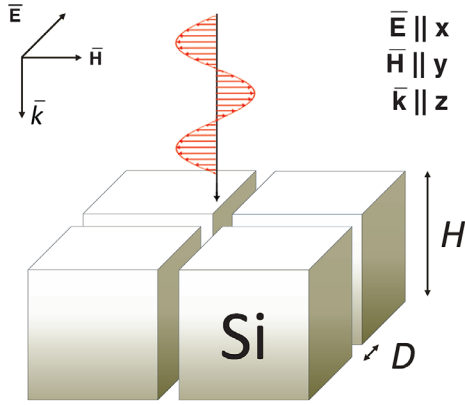


Figure 1. The artistic representation of the quadrumer of silicon cubes.

one needs to increase particles volume to excite high-order multipoles (magnetic octupole, electric 16-pole, etc.). However, exploiting bigger particles as building blocks is complicated because their size and, consequently, interparticle spacing can surpass resonant wavelengths. That results in a diffraction, which crucially restricts the functionality of metasurfaces making them to become simple diffraction lattices. Here we pave a way to overcoming this challenge and demonstrate the possibility to resonantly excite high-order multipoles via artificial nanostructuring of a scatterer, so that its total size remains nearly unchanged and effectively smaller than the resonant wavelength. This approach can find wide application for the development of new types of metasurfaces, compact nanoantennas with unique high-order multipole response, and other nanostructures for multiscale light governing. In general, tailoring the resonant response of high-order multipole moments over the optical spectral range opens new opportunities in practical applications, for example, sensors, detectors, and selective or directive nanoantennas.

2. Theoretical Background

Here, we use multipole decomposition approach described in refs. [13,45–47] including multipole moments up to the magnetic octupole (MOCT) term. To study the multipole contributions to a scattering cross section of full quadrumer structure presented in **Figure 1** we consider it as an unite system. The origin of the Cartesian coordinate system is located at the center of mass (center of symmetry) of the structure, and, for the incident wave, the electric field is polarized along x -axis, and k -vector is directed along z -axis (see **Figure 1**).

In our approximation a scattering cross section of a particle in a homogeneous host medium can be presented as (see ref. [47] for details)

$$C_{\text{sca}} \simeq \frac{k_0^4}{6\pi\epsilon_0^2|\mathbf{E}_{\text{inc}}|^2}|\mathbf{D}|^2 + \frac{k_0^4\epsilon_d\mu_0}{6\pi\epsilon_0|\mathbf{E}_{\text{inc}}|^2}|\mathbf{m}|^2 + \frac{k_0^6\epsilon_d}{720\pi\epsilon_0^2|\mathbf{E}_{\text{inc}}|^2}|\hat{Q}|^2 + \frac{k_0^6\epsilon_d^2\mu_0}{80\pi\epsilon_0|\mathbf{E}_{\text{inc}}|^2}|\hat{M}|^2 + \frac{k_0^8\epsilon_d^2}{1890\pi\epsilon_0^2|\mathbf{E}_{\text{inc}}|^2}|\hat{O}|^2 + \frac{k_0^8\epsilon_d^3\mu_0}{1890\pi k_0^8\epsilon_0|\mathbf{E}_{\text{inc}}|^2}|\hat{O}_m|^2 \quad (1)$$

where \mathbf{E}_{inc} is the electric field amplitude of the incident light wave, $\epsilon_d = n_d^2$ is the dielectric permittivity of the surrounding medium, ϵ_0 is the vacuum electric permittivity, and $v_d = c/\sqrt{\epsilon_d}$ is the light speed in the surrounding medium; k_0 and k_d are the wavenumbers in vacuum and in the surrounding medium, correspondingly. \mathbf{m} is the magnetic dipole moment (MD) of a particle; \mathbf{D} is the total electric dipole moment (TED); \hat{Q} , \hat{M} , \hat{O} , and \hat{O}_m are the electric quadrupole tensor (EQ), the magnetic quadrupole tensor (MQ), the tensor of electric octupole (OCT), and the tensor of magnetic octupole (MOCT), respectively. Here $\|\|$ denotes the sum of squared tensor components. Note that these tensors are symmetric and traceless, and in tensor notation, for example, \hat{Q} is equal to $Q_{\alpha\beta}$ (for quadrupole moments) and \hat{O} is equal to $O_{\alpha\beta\gamma}$ (for octupole moments), where subscript indices denote components (e.g., $\alpha = x, y, z$).^[45] Let us also show the expressions used here for the Cartesian electric and magnetic octupole moments, expanding the multipole decomposition at ref. [46]

$$\hat{O} = \frac{15i}{\omega} \int_{V_s} \frac{j_2(k_d r')}{(k_d r')^2} (\mathbf{j}\mathbf{r}' + \mathbf{r}'\mathbf{j}\mathbf{r}' + \mathbf{r}'\mathbf{r}'\mathbf{j} - \hat{A}) d\mathbf{r}' \quad (2)$$

$$\hat{O}_m = \frac{105}{4} \int_{V_s} \frac{j_3(k_d r')}{(k_d r')^3} ([\mathbf{r}' \times \mathbf{j}]\mathbf{r}' + \mathbf{r}'[\mathbf{r}' \times \mathbf{j}]\mathbf{r}' + \mathbf{r}'\mathbf{r}'[\mathbf{r}' \times \mathbf{j}] - \hat{A}') d\mathbf{r}' \quad (3)$$

where vector $\mathbf{j}(\mathbf{r}')$ is the electric polarization current density depending on the position inside the scatterer and induced by an incident light wave, \mathbf{r}' is the radius vector of a point inside the scatterer, ω is the angular frequency of the incident wave; $j_2(k_d r')$, $j_3(k_d r')$ are the spherical Bessel functions, V_s is a scatterer volume, and the tensors \hat{A} and \hat{A}' are

$$A_{\beta\gamma\tau} = \delta_{\beta\gamma} V_\tau + \delta_{\beta\tau} V_\gamma + \delta_{\gamma\tau} V_\beta \quad (4)$$

$$A'_{\beta\gamma\tau} = \delta_{\beta\gamma} V'_\tau + \delta_{\beta\tau} V'_\gamma + \delta_{\gamma\tau} V'_\beta \quad (5)$$

where $\beta = x, y, z$; $\gamma = x, y, z$; $\tau = x, y, z$; $\delta_{\beta\gamma}$ is the Kronecker delta,

$$\mathbf{V} = \frac{1}{5}[2(\mathbf{r}' \cdot \mathbf{j})\mathbf{r}' + r'^2\mathbf{j}] \quad (6)$$

$$\mathbf{V}' = \frac{1}{5}r'^2[\mathbf{r}' \times \mathbf{j}] \quad (7)$$

The combinations of three vectors (like $\mathbf{j}\mathbf{r}'$) in Equations (2) and (3) are the tensor products of the corresponding vectors, the sign \times stands for the vector product and the sign \cdot stands for the scalar product of two vectors. Detailed derivations are presented in ref. [47].

The polarization currents inside the dielectric structure are calculated using the total electric field obtained from the full-wave simulations in the commercial package COMSOL Multiphysics.^[48] The details of the methods involved can be found, for example, in ref. [49]. Electric fields $\mathbf{E}(\mathbf{r}')$ and polarization currents are related by the Equation $\mathbf{j}(\mathbf{r}') = -i\omega\epsilon_0(\epsilon_s - \epsilon_d)\mathbf{E}(\mathbf{r}')$, where ϵ_s is the dielectric permittivity of the silicon scatterers.^[35] These currents are then used to obtain multipole contributions to the scattering cross section. To compare, the total

scattering cross section is also obtained through the direct integration of the Poynting vector over a closed surface in the far-field zone and the normalization to the incident field intensity.

3. Results and Discussion

In this work, we study previously unrevealed MOCT-induced optical properties of silicon quadrumers. We learn how to use controllable resonant MOCT excitation to tailor magnetic hot-spots and resonant energy absorption. The considered systems are the silicon block with dimensions equal to $500 \times 500 \times 250$ nm, which represents zero distance between silicon cubes in Figure 1 and silicon quadrumers composed of four Si cubes ($250 \times 250 \times 250$ nm) with distance between them $D = 25, 50$, and 100 nm. These structures are illuminated with a linearly polarized monochromatic plane wave with time-dependence $e^{-i\omega t}$ as shown in Figure 1. Material data for silicon has been taken from ref. [35]. To investigate scattering cross section spectral resonances, we apply the multipole decomposition technique which shows good performance in all cases considered (Figure 2). The almost perfect agreement between the sum of the multipole contributions and the directly calculated scattered cross section proves that the multipole approach is sufficiently accurate. Figure 2a shows the scattering cross section spectrum calculated for the solid silicon block. One can note that both the resonant multipole contributions and the total scattering cross section in this case significantly differ from the spectra in Figure 2b–d due to the introduction of inhomogeneity to the system.

In this way, the conversion of the solid block to the quadramer structure leads to a strong reconfiguration of electric and magnetic fields in the system and to a higher order multipole excitation. Surprisingly, the presence of narrow air gaps in the quadramer leads to the excitation of the MOCT moment in the considered spectral range. Note that this is not related to the increase in the total structure size, since our calculations for solid blocks with the edge of 525 nm do not show MOCT resonances in the considered spectral range. To visualize this, we show the total scattering cross section of $525 \times 525 \times 250$ nm silicon block (dashed line in Figure 2b) in order to compare it with the case of the corresponding quadramer. It can be seen that there is no resonant response between $\lambda = 850$ nm and $\lambda = 900$ nm; small resonant peak at $\lambda = 840$ nm corresponds to EQ.

Let us consider in detail the resonant excitation of the magnetic octupole moment at the wavelengths of 850 – 900 nm. Cutting the solid block enables MOCT resonance weakening with increasing the intercubes distance. The resonant MOCT peak occurs at $\lambda = 874$ nm in Figure 2b, at $\lambda = 863$ nm in Figure 2c, and at $\lambda = 852$ nm in Figure 2d. While attenuating, the resonant peak also experiences a blue shift. Moreover, the multipole decomposition and scattering cross section do not depend on rotation of the incident plane wave polarization by 45° (not demonstrated in figures).

Figure 3 shows the distribution of normalized (to the magnetic field amplitude of the incident wave) magnetic field at the MOCT resonance. It is important for practical applications to be able to create the so-called magnetic hot-spots in free space.^[42] Due to structuring, the total magnetic field in the gaps can be enhanced (comparing to the incident one) up to ≈ 10 times for $D = 50$ nm (Figure 3a) and ≈ 14 times for $D = 25$ nm (Figure 3b). Strong

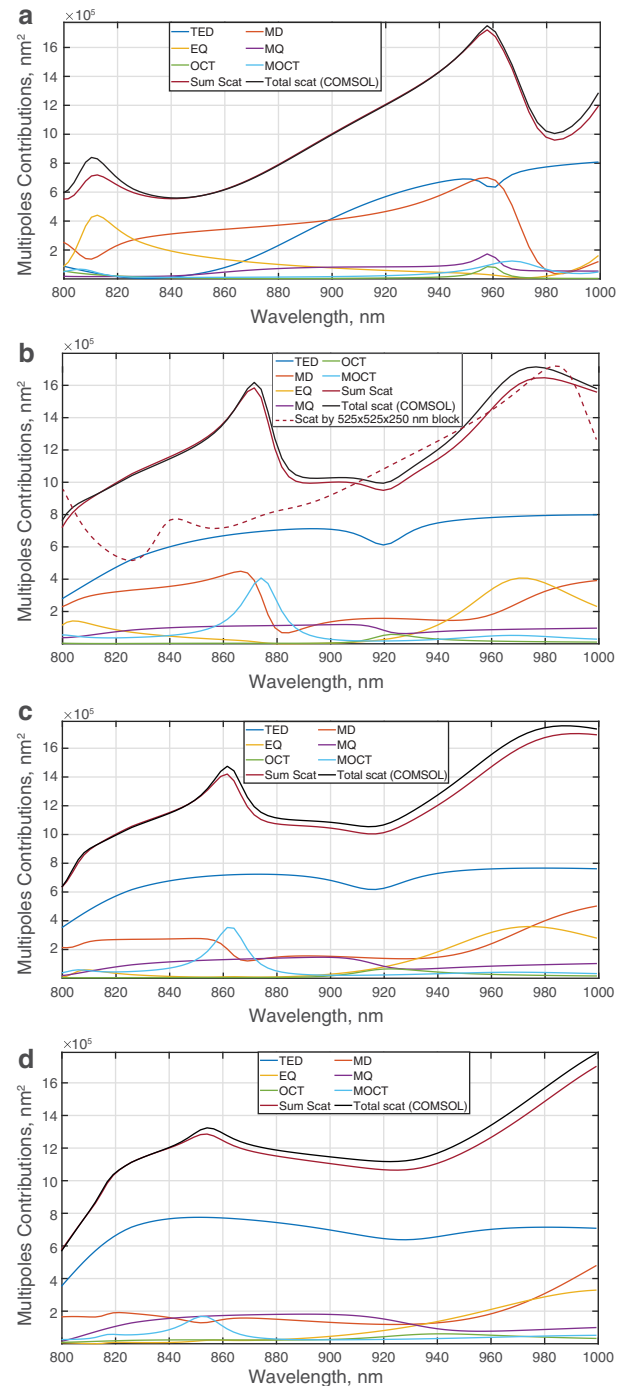


Figure 2. Scattering cross-section spectra and corresponding multipole contributions calculated for a) the single silicon block of height $H = 250$ nm and base edge 500 nm; b–d) the quadramer of silicon cubes. The distance between cubes in the quadramer is b) $D = 25$ nm c) $D = 50$ nm d) $D = 100$ nm. 'Sum Scat' states for the scattering cross section as the sum of the multipole contributions; 'Total scat (COMSOL)' states for the total scattering cross sections calculated directly in COMSOL.

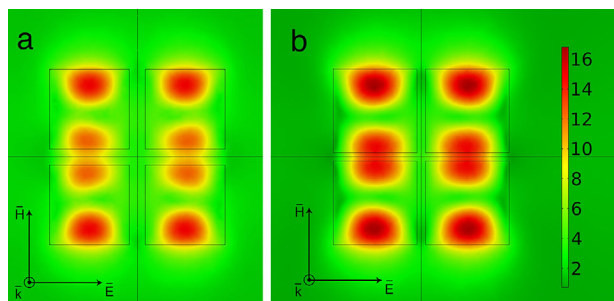


Figure 3. a) Distribution of the normalized magnetic field in (xy) - plane ($z = 0$) of the silicon quadramer with a) $D = 50$ nm, $\lambda = 863$ nm, b) $D = 25$ nm, $\lambda = 874$ nm. Color bar is the same for both pictures.

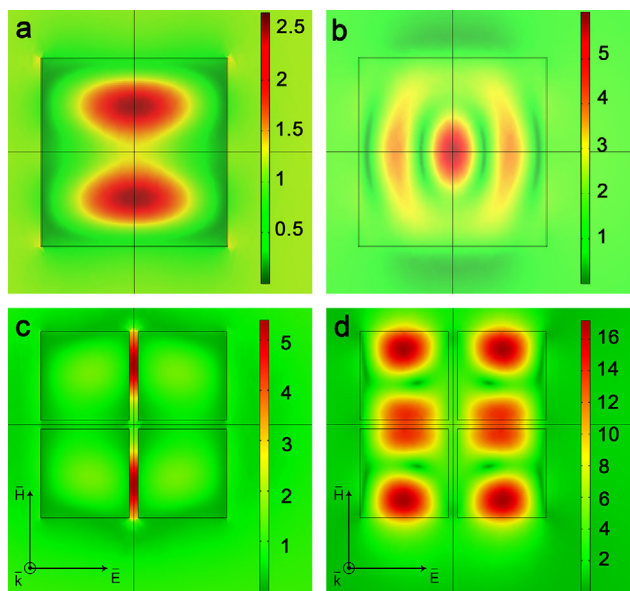


Figure 4. The absolute value of a,c) E_x and b,d) H_y in a,b) the solid silicon block and c,d) the silicon quadramer with $D = 25$ nm at $\lambda = 874$ nm.

local magnetic fields can be used to control or detect small quantum objects (quantum dots, atoms, and molecules) supporting magnetic optical transitions.^[50] Magnetic hot-spots are also useful for spectroscopy,^[51] better enhancement of Raman scattering, fluorescence, and circular dichroism of molecules,^[52] sensing,^[53] and other applications.

The location of obtained hot-spots can also be tuned using the incident light polarization. The hot-spots move to another air gaps if the polarization is rotated by 90° (i.e., if electric field is polarized along perpendicular axis). It is possible to exploit this effect to design magnetic switchers at the nanoscale.

It is important to go in details with the physics of the considered process. **Figure 4a,c** show the absolute value of the x -component of the electric field (E_x) in the solid block and in the quadramer, respectively. Following Maxwell's equations, in the oligomer structure the electric field enhancement appears in the slits along the polarization of the incident wave due to the discontinuity of the normal component. In addition, **Figure 4b,d** show the absolute value of the y -component of the magnetic field (H_y) and the crucial redistribution of the magnetic field because of the structuring. This leads to six different field concentration zones

in the quadramer structure constructing magnetic octupole near-field pattern.^[34] The magnetic field does not undergo a discontinuity in the gaps along H_y ($\mu = 1$ in the both media) that is why the magnetic hot-spots take place between the cubes too.

In addition to the magnetic field enhancement, MOCT resonance can provide a strong electromagnetic absorption in the quadramer. **Figure 5a** shows the comparison of absorbed power for λ between 850 and 900 nm for the solid silicon block and the quadramer with the distance $D = 25$ nm between the cubes. **Figure 5b** proves that the discovered energy absorption peak spectrally corresponds to the MOCT resonance. It is worth noting that in this spectral range natural light absorption by silicon is small. Therefore, air gaps in the quadramer structure cause strong absorption in silicon, despite its very small $Im(n) \approx 0.08$. **Figure 5c** compares the electric field inside the silicon block and quadramer structure. Clearly, resonant magnetic octupole response leads to a strong electric field concentration and, therefore, to the resonant absorption in the silicon quadramer. The spectral position of the MOCT resonance and, hence, the position of the absorption peak can be changed by varying the distance between the cubes. Such the tunable absorption can be widely used to control the energy concentration by dielectric structures and to design modern optical devices.

Here, we note that the substrate influence on this effect is yet to be studied. It is known that dielectric substrates with low refractive index almost does not change the optical response,^[7,54] however, to take into account more reflective materials more complex formalism should be introduced. The principal demonstration paved the way to future theoretical and experimental investigations of magnetic octupole excitations in quadramers placed on different metal and dielectric substrates.

4. Conclusion

In this work we study resonant MOCT excitation which leads to controlled magnetic hot-spots and resonant absorption by a nanostructure. We analyze the multipole contributions to the scattering cross section and reveal the excitation of magnetic octupole due to the coupling effects in this structure as compared to the single cube. In this work, the resonant excitation of a magnetic octupole moment in dielectric quadramers is demonstrated and analyzed in detail. We show how to control MOCT resonant excitation and its spectral position. In addition, we reveal its possible application to obtain magnetic hot-spots and to absorb electromagnetic energy in the nanostructure. The magnetic field in the air gap between the nanocubes can be 14 times larger in comparison with incident one, and is even stronger inside the nanostructure. Use of quadramers as building blocks for metasurfaces promises even higher magnetic field enhancement due to potential excitation of so-called trapped modes. It is very important to note that an excitation of high-order multipole moments exploiting nanostructuring of small particles is the powerful approach to avoid diffraction restriction in designing of advanced metasurfaces and metamaterials. Moreover, after being scaled to the microwave region the considered structure could be very perspective for magnetic resonance imaging applications, where a strong concentration of magnetic fields is necessary to increase the contrast and quality of the pictures.^[55,56] Besides,

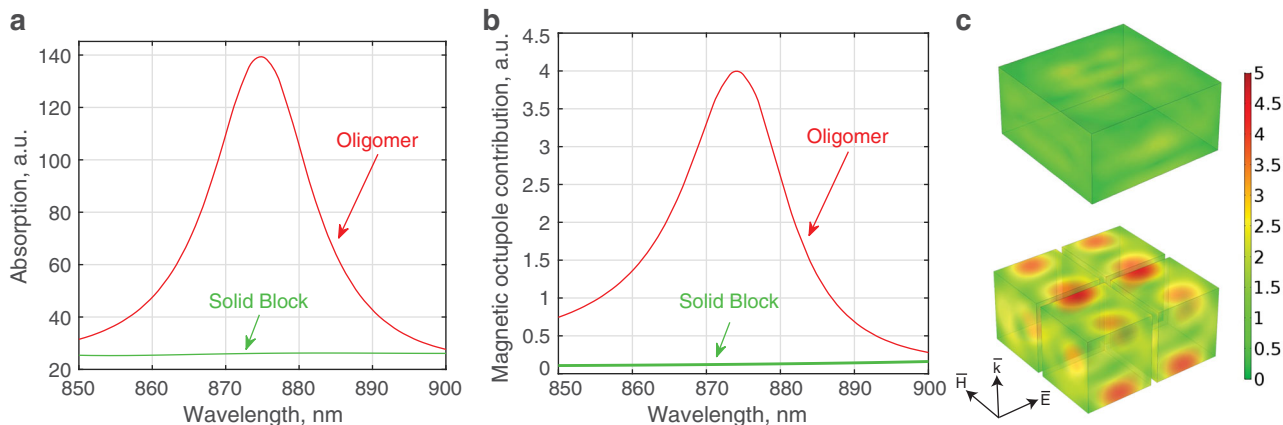


Figure 5. Spectra of the a) absorption power and b) MOCT contribution to the scattering cross section calculated for a single silicon block of height $H = 250$ nm and base edge 500 nm (green lines) and the quadrumer of silicon cubes with the distance between cubes $D = 25$ nm (red lines). The absorption peak in the structure clearly corresponds to the resonant excitation of MOCT moment. c) Normalized electric field inside the solid block (top) and quadrumer (bottom) at $\lambda = 874$ nm. One can see that resonant MOCT response provides strong electric field concentration leading to the resonant absorption in the silicon quadrumer.

resonant magnetic octupole response can be widely used for spectroscopy, sensing, small quantum objects detection, and many other promising applications.^[57–61]

Acknowledgements

The authors thank Svetlana Korinfskaya for help with the artistic work. This work was supported by the Israel Innovation Authority-Kamin Program, Grant. No. 62045 (Year 2). A.S.S. acknowledges the support of the Russian Fund for Basic Research within the projects 18-02-00414, 18-52-00005. The development of the analytical approach was partially supported by the Russian Science Foundation Grant No. 18-19-00684. Support from the the Russian Fund for Basic Research within the projects 18-29-02089 is acknowledged as well. Contribution of P.D.T. in the research was performed as a part of the joint Ph.D. program between the BGU and ITMO.

Conflict of Interest

The authors declare no conflict of interest.

Keywords

magnetic hot-spots, magnetic octupole, oligomers, quadrumers, silicon photonics

Received: October 1, 2019

Revised: January 26, 2020

Published online:

- [1] I. Staude, J. Schilling, *Nat. Photonics* **2017**, *11*, 274.
- [2] Y. Kivshar, *Natl. Sci. Rev.* **2018**, *5*, 144.
- [3] S. M. Kamali, E. Arbabi, A. Arbabi, A. Faraon, *Nanophotonics* **2018**, *7*, 1041.
- [4] A. B. Evlyukhin, C. Reinhardt, A. Seidel, B. S. Luk'yanchuk, B. N. Chichkov, *Phys. Rev. B* **2010**, *82*, 045404.

- [5] A. B. Evlyukhin, C. Reinhardt, B. N. Chichkov, *Phys. Rev. B* **2011**, *84*, 235429.
- [6] A. B. Evlyukhin, S. M. Novikov, U. Zywieta, R. L. Eriksen, C. Reinhardt, S. I. Bozhevolnyi, B. N. Chichkov, *Nano Lett.* **2012**, *12*, 3749.
- [7] U. Zywieta, A. B. Evlyukhin, C. Reinhardt, B. N. Chichkov, *Nat. Commun.* **2014**, *5*, 3402.
- [8] A. E. Miroshnichenko, A. B. Evlyukhin, Y. F. Yu, R. M. Bakker, A. Chipouline, A. I. Kuznetsov, B. Luk'yanchuk, B. N. Chichkov, Y. S. Kivshar, *Nat. Commun.* **2015**, *6*, 8069.
- [9] A. A. Basharin, M. Kafesaki, E. N. Economou, C. M. Soukoulis, V. A. Fedotov, V. Savinov, N. I. Zheludev, *Phys. Rev. X* **2015**, *5*, 011036.
- [10] J. B. Khurgin, *Nat. Nanotechnol.* **2015**, *10*, 2.
- [11] A. Karabchevsky, A. Mosayyebi, A. V. Kavokin, *Light: Sci. Appl.* **2016**, *5*, e16164.
- [12] A. Karabchevsky, O. Krasnykov, M. Auslender, B. Hadad, A. Goldner, I. Abdulhalim, *Plasmonics* **2009**, *4*, 281.
- [13] R. Alaei, C. Rockstuhl, I. Fernandez-Corbaton, *Adv. Opt. Mater.* **2019**, *7*, 1800783.
- [14] Y. Yang, A. E. Miroshnichenko, S. V. Kostinski, M. Odit, P. Kapitanova, M. Qiu, Y. S. Kivshar, *Phys. Rev. B* **2017**, *95*, 165426.
- [15] I. Staude, A. E. Miroshnichenko, M. Decker, N. T. Fofang, S. Liu, E. Gonzales, J. Dominguez, T. S. Luk, D. N. Neshev, I. Brener, Y. Kivshar, *ACS Nano* **2013**, *7*, 7824.
- [16] P. D. Terekhov, K. V. Baryshnikova, A. S. Shalin, A. Karabchevsky, A. B. Evlyukhin, *Opt. Lett.* **2017**, *42*, 835.
- [17] W. Chen, Y. Chen, W. Liu, *Laser Photonics Rev.* **2019**, *13*, 1900067.
- [18] P. Grah, A. Shevchenko, M. Kaivola, *New J. Phys.* **2012**, *14*, 093033.
- [19] P. D. Terekhov, V. E. Babicheva, K. V. Baryshnikova, A. S. Shalin, A. Karabchevsky, A. B. Evlyukhin, *Phys. Rev. B* **2019**, *99*, 045424.
- [20] S. Mühlig, C. Menzel, C. Rockstuhl, F. Lederer, *Metamaterials* **2011**, *5*, 64.
- [21] M.-T. Suzuki, T. Nomoto, R. Arita, Y. Yanagi, S. Hayami, H. Kusunose, *Phys. Rev. B* **2019**, *99*, 174407.
- [22] I. M. Hancu, A. G. Curto, M. Castro-López, M. Kuttge, N. F. van Hulst, *Nano Lett.* **2013**, *14*, 166.
- [23] H. K. Shamkhi, K. V. Baryshnikova, A. Sayanskiy, P. Kapitanova, P. D. Terekhov, P. Belov, A. Karabchevsky, A. B. Evlyukhin, Y. Kivshar, A. S. Shalin, *Phys. Rev. Lett.* **2019**, *122*, 193905.
- [24] B. Luk'yanchuk, R. Paniagua-Domínguez, A. I. Kuznetsov, A. E. Miroshnichenko, Y. S. Kivshar, *Phys. Rev. A* **2017**, *95*, 063820.

- [25] V. Savinov, V. Fedotov, N. I. Zheludev, *Phys. Rev. B* **2014**, *89*, 205112.
- [26] D. A. Powell, *Phys. Rev. Appl.* **2017**, *7*, 034006.
- [27] P. Terekhov, K. Baryshnikova, A. Evlyukhin, A. Shalin, *J. Phys.: Conf. Ser.* **2017**, *929*, 012065.
- [28] M. Balezin, K. V. Baryshnikova, P. Kapitanova, A. B. Evlyukhin, *J. Appl. Phys.* **2018**, *124*, 034903.
- [29] P. D. Terekhov, K. V. Baryshnikova, Y. A. Artemyev, A. Karabchevsky, A. S. Shalin, A. B. Evlyukhin, *Phys. Rev. B* **2017**, *96*, 035443.
- [30] A. Y. Zhu, W. T. Chen, A. Zaidi, Y.-W. Huang, M. Khorasaninejad, V. Sanjeev, C.-W. Qiu, F. Capasso, *Light: Sci. Appl.* **2018**, *7*, 17158.
- [31] W. Liu, A. E. Miroschnichenko, *ACS Photonics* **2017**, *5*, 1733.
- [32] P. Terekhov, H. Shamkhi, E. Gurvitz, K. Baryshnikova, A. Evlyukhin, A. Shalin, A. Karabchevsky, *Opt. Express* **2019**, *27*, 10924.
- [33] R. Alaei, M. Albooyeh, S. Tretyakov, C. Rockstuhl, *Opt. Lett.* **2016**, *41*, 4099.
- [34] E. A. Gurvitz, K. S. Ladutenko, P. A. Dergachev, A. B. Evlyukhin, A. E. Miroschnichenko, A. S. Shalin, *Laser Photonics Rev.* **2019**, *13*, 1800266.
- [35] E. D. Palik, *Handbook of Optical Constants of Solids: Handbook of Thermo-Optic Coefficients of Optical Materials with Applications*, Elsevier, New York **1997**.
- [36] L. Wang, Y. Rho, W. Shou, S. Hong, K. Kato, M. Eliceiri, M. Shi, C. P. Grigoropoulos, H. Pan, C. Carraro, D. Qi, *ACS Nano* **2018**, *12*, 2231.
- [37] F. Deng, H. Liu, M. Panmai, S. Lan, *Opt. Express* **2018**, *26*, 20051.
- [38] P. D. Terekhov, K. V. Baryshnikova, Y. Greenberg, Y. H. Fu, A. B. Evlyukhin, A. S. Shalin, A. Karabchevsky, *Sci. Rep.* **2019**, *9*, 3438.
- [39] P. M. Voroshilov, C. R. Simovski, P. A. Belov, A. S. Shalin, *J. Appl. Phys.* **2015**, *117*, 203101.
- [40] A. Katiyi, A. Karabchevsky, *ACS Sens.* **2018**, *3*, 618.
- [41] Y. Galutin, E. Falek, A. Karabchevsky, *Sci. Rep.* **2017**, *7*, 12076.
- [42] K. V. Baryshnikova, A. Novitsky, A. B. Evlyukhin, A. S. Shalin, *J. Opt. Soc. Am. B* **2017**, *34*, D36.
- [43] R. M. Bakker, D. Permyakov, Y. F. Yu, D. Markovich, R. Paniagua-Dominguez, L. Gonzaga, A. Samusev, Y. Kivshar, B. Luk'yanchuk, A. I. Kuznetsov, *Nano Lett.* **2015**, *15*, 2137.
- [44] A. Rahimzadegan, D. Arslan, D. Dams, A. Groner, X. Garcia-Santiago, R. Alaei, I. Fernandez-Corbaton, T. Pertsch, I. Staude, C. Rockstuhl, *Nanophotonics* **2020**, *9*, 75.
- [45] A. B. Evlyukhin, T. Fischer, C. Reinhardt, B. N. Chichkov, *Phys. Rev. B* **2016**, *94*, 205434.
- [46] R. Alaei, C. Rockstuhl, I. Fernandez-Corbaton, *Opt. Commun.* **2018**, *407*, 17.
- [47] A. B. Evlyukhin, B. N. Chichkov, *Phys. Rev. B* **2019**, *100*, 125415.
- [48] COMSOL Multiphysics® v.5.4. www.comsol.com. COMSOL AB, Stockholm, Sweden.
- [49] W. B. Zimmerman, *Multiphysics Modeling with Finite Element Methods*, Vol. 18, World Scientific, Singapore **2006**.
- [50] C. L. Degen, F. Reinhard, P. Cappellaro, *Rev. Mod. Phys.* **2017**, *89*, 035002.
- [51] M. Sadrara, M. Miri, *Sci. Rep.* **2019**, *9*, 2926.
- [52] Z. Naeimi, M. Miri, *Opt. Lett.* **2018**, *43*, 462.
- [53] Z. Yong, S. Zhang, C. Gong, S. He, *Sci. Rep.* **2016**, *6*, 24063.
- [54] P. Spinelli, M. Verschuuren, A. Polman, *Nat. Commun.* **2012**, *3*, 692.
- [55] A. Andreychenko, H. Kroeze, D. W. Klomp, J. J. Lagendijk, P. R. Luijten, C. A. van den Berg, *Magn. Reson. Med.* **2013**, *70*, 875.
- [56] A. A. Mikhailovskaya, A. V. Shchelokova, D. A. Dobrykh, I. V. Sushkov, A. P. Slobozhanyuk, A. Webb, *J. Magn. Reson.* **2018**, *291*, 47.
- [57] M. Kasperczyk, S. Person, D. Ananias, L. D. Carlos, L. Novotny, *Phys. Rev. Lett.* **2015**, *114*, 163903.
- [58] T. H. Taminiau, S. Karaveli, N. F. Van Hulst, R. Zia, *Nat. Commun.* **2012**, *3*, 979.
- [59] H. Giessen, R. Vogelgesang, *Science* **2009**, *326*, 529.
- [60] M. Burrelli, D. Van Oosten, T. Kampfrath, H. Schoenmaker, R. Heide-man, A. Leinse, L. Kuipers, *Science* **2009**, *326*, 550.
- [61] O. Borovkova, D. Ignatyeva, S. Sekatskii, A. Karabchevsky, V. Belotelov, *Photonics Res.* **2020**, *8*, 57.